

Majorana molecules and their spectral fingerprints

J. E. Sanches ¹, L. S. Ricco,¹ Y. Marques,² W. N. Mizobata ¹, M. de Souza,³ I. A. Shelykh,^{2,4} and A. C. Seridonio ^{1,3,*}

¹*Department of Physics and Chemistry, São Paulo State University (Unesp), School of Engineering, 15385-000, Ilha Solteira-SP, Brazil*

²*Department of Physics, ITMO University, St. Petersburg 197101, Russia*

³*Department of Physics, São Paulo State University (Unesp), IGCE, 13506-970, Rio Claro-SP, Brazil*

⁴*Science Institute, University of Iceland, Dunhagi-3, IS-107, Reykjavik, Iceland*



(Received 1 April 2020; accepted 3 August 2020; published 19 August 2020)

We introduce the concept of a Majorana molecule, a topological bound state appearing in the geometry of a double quantum dot structure flanking a topological superconducting nanowire. We demonstrate that, if the Majorana bound states at opposite edges are probed nonlocally in a two-probe experiment, the spectral density of the system reveals the so-called *half-bowtie* profiles, while Andreev bound states become resolved into bonding and antibonding molecular configurations. We reveal that this effect is due to the Fano interference between *pseudospin* superconducting pairing channels, and we propose that it can be captured by a *pseudospin* resolved scanning tunneling microscope tip.

DOI: [10.1103/PhysRevB.102.075128](https://doi.org/10.1103/PhysRevB.102.075128)

I. INTRODUCTION

The recent decade witnessed the increasing interest of the condensed-matter community in Majorana physics. In particular, the concept of Majorana bound states (MBSs) as promising building blocks for topologically protected and fault-tolerant quantum computing received special attention [1–6]. MBSs are zero-modes appearing at topological boundaries of condensed-matter systems with spinless *p*-wave superconductivity, as was first predicted by Kitaev in his seminal work [7]. They manifest themselves via zero-bias peak (ZBP) signature in local conductance measurements [8]. As candidates for hosting nonlocal MBSs, such material platforms as ferromagnetic atomic chains [9–19] and semiconductor hybrid nanowires [8,20–23] were proposed. Isolated MBSs are also supposed to be attached to cores of superconducting vortices [24,25].

Interestingly enough, the Majorana quasiparticle detection can be done by determining transport quantities through a single quantum dot (QD) [26–36]. As examples, we highlight the electrical shot-noise [30–33] and the thermoelectric properties [34–36]. Although the former cannot fully trace the QD density of states (DOS), it is especially helpful in introducing a full counting statistics of charge tunneling events, which is unique for Majorana systems [30]. Further, the shot-noise enables us to distinguish a nontopological ZBP from the corresponding topological ZPB [31]. It also reveals that the fractional value of the effective charge, by means of current fluctuations, thus depends on the system bias-voltage [32]. Additionally, the differential quantum noise shows that the photon absorbed spectra by a MBS show a universal behavior, being frequency- and bias-voltage-independent [33].

Similarly, the zero-bias limit of the thermoelectric properties presents striking features. The thermopower enhancement [34,35], and according to some of us the possibility of a tuner of heat and charge assisted by MBSs [36], are just a few examples of such features.

Astonishingly, upon attaching an extra QD, the control of the MBS leakage [27] into QDs becomes feasible [37,38]. According to Cifuentes *et al.* [37], in several geometric arrangements of QDs, known as “parallel,” “in-series,” and “T-shaped,” the spatial manipulation of an MBS is allowed. On the grounds of the *pseudospin*, this switching is revealed as the cornerstone for the Majorana fermion *qubit* cryptography, as proposed in Ref. [38] by some of us. This cryptography arises from the delicate interplay between Fano interference [39,40] and topological superconductivity.

It is noteworthy that the *pseudospin* has been guided by the interpretation of the transport through spinless two-level QD and double-QD systems [41–43]. Especially in the latter, the Kondo effect is induced by an interdot Coulomb correlation [43]. It is worth mentioning that the *pseudospin* consists of mapping the system orbital degrees of freedom into those equivalent to the *z*-components of its spin $\frac{1}{2}$ counterpart, i.e., by projecting them along the quantization of the *pseudospin* axis [41]. We highlight the fact that these peculiar degrees of freedom are experimentally detectable by *pseudospin*-resolved transport spectroscopy [44].

Concerning the Fano interference in the presence of MBSs and QDs with a plethora of intriguing characteristics [45–54], special attention should be paid to the findings of Ref. [47] by Xia *et al.* Their results reveal that the conductance through two QDs obeys in an elegant manner, and within the low-bias-voltage limit, a Fano-like expression [39,40]. Surprisingly, this expression is characterized by QD-wire couplings and a Fano parameter of interference, which is dependent upon the MBSs overlapping. Therefore, such an analysis offers an attractive experimental strategy, clearly supported by the

*Author to whom all correspondence should be addressed: antonio.seridonio@unesp.br

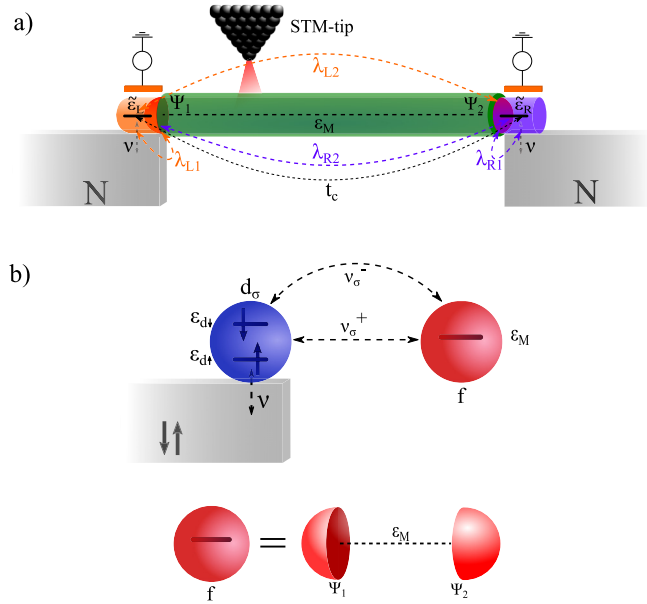


FIG. 1. (a) The sketch of the considered system with a pseudospin resolved STM-tip acting as a probe of the one-dimensional topological superconductor (1D-TSC) and nonlocal Majorana bound states (MBSs) $\Psi_j = \Psi_j^\dagger$ ($j = 1, 2$) at the edges and flanked by a pair of QDs, with energies $\tilde{\epsilon}_L$ and $\tilde{\epsilon}_R$ coupled to metallic leads, via the hybridization \mathcal{V} . The nonlocal MBSs couple to the QDs via the amplitudes $\lambda_{\alpha j}$ ($\alpha = L, R$) and to each other by the overlap term ϵ_M . The system is characterized by spinless and p -wave superconductivity, due to the large Zeeman splitting. (b) Mapping of the original system into equivalent geometry with a single QD with pseudospin degrees of freedom. The amplitudes \mathcal{V}_σ^+ refer to the pseudospin pairing channels of the formation of Cooper pairs spatially split into the orbitals ($d_\sigma f$) with energies $\epsilon_{d\sigma}$ and ϵ_M . The terms \mathcal{V}_σ^- stand for pseudospin ballistic transport processes through such orbitals. The nonlocal orbital f is formed by a pair of the MBSs.

Fano effect, in recognizing MBSs far apart in superconducting wires, as well as in estimating how topological are these MBSs.

In this work, distinct from Refs. [37,38,47], by including the nonlocality degree of MBSs [28] we propose the concept of a Majorana molecule within the *pseudospin* framework [41–43]. It is worth noting that such a nonlocality feature is a key ingredient for reproducing experimental results [23,28]. Then, this molecule appears in a configuration similar to those considered at the end of Ref. [23], but with spectral fingerprints probed by a *pseudospin*-resolved scanning tunneling microscope (STM) tip, similarly to Ref. [29] and schematically shown in Fig. 1(a) of the current paper. It consists of a one-dimensional (1D) topological superconductor (TSC) hosting MBSs at the edges, which hybridize with normal fermionic states of a pair of QDs flanking the TSC wire, placed in the strong longitudinal magnetic field. If the latter is strong enough, so that Zeeman splitting becomes much larger than all other characteristic energies of the system, the *spinless* condition is fulfilled. In this case, the tuning of the parameters of the system leads to a crossover between the well-known regime of individual Andreev bound states (ABSs) [23] (*the Majorana molecule turned off*), and the

regime in which one witnesses the splitting of the ABS into bonding and antibonding molecular configurations (*the Majorana molecule turned on*). The formation of these states can be described in terms of the so-called *pseudospins* (\uparrow , \downarrow), which determine the structure of the QDs orbitals by means of superconducting pairings in these channels. Note that, contrary to the single QD geometry considered before [23,28], in our setup the QDs act as a nonlocal two-probe detector that captures the Fano interference effects between various tunneling paths, including those involving the MBSs.

We demonstrate that, similar to what happens in the system of a pair of QDs placed within a semiconductor [55] or a Dirac-Weyl semimetal host [56,57], the Fano effect in the considered system defines the novel type of molecular binding of QD orbitals, and leads to the formation of a Majorana molecule, characterized by the so-called *half-bowtie* profiles in the spectral density of states.

II. THE MODEL

The geometry we consider is shown in Fig. 1(a). The system under study consists of an STM-tip perturbatively coupled to the 1D-TSC nanowire with nonlocal MBSs formed at its edges and flanked by a pair of QDs, where the latter are attached to metallic leads. We suggest that the external magnetic field applied along the direction of the wire is large enough so that only spin-up states lie below the Fermi energy, and spin-down states can be just totally excluded from consideration [26,27,36]. We account for the possible coupling between MBSs localized at the opposite edges of the TSC wire, which can change their nonlocality degree and lead to the crossover between highly nonlocal MBSs and more local ABSs.

The Hamiltonian of the system reads

$$\begin{aligned} \mathcal{H} = & \sum_{\alpha\mathbf{k}} \epsilon_{\alpha\mathbf{k}} \tilde{c}_{\alpha\mathbf{k}}^\dagger \tilde{c}_{\alpha\mathbf{k}} + \sum_{\alpha} \tilde{\epsilon}_{\alpha} \tilde{d}_{\alpha}^\dagger \tilde{d}_{\alpha} + t_c (\tilde{d}_L^\dagger \tilde{d}_R + \text{H.c.}) \\ & + \mathcal{V} \sum_{\alpha\mathbf{k}} (\tilde{c}_{\alpha\mathbf{k}}^\dagger \tilde{d}_{\alpha} + \text{H.c.}) + \lambda_{L1} (\tilde{d}_L - \tilde{d}_L^\dagger) \Psi_1 \\ & + i\lambda_{L2} (\tilde{d}_L + \tilde{d}_L^\dagger) \Psi_2 + i\lambda_{R1} (\tilde{d}_R + \tilde{d}_R^\dagger) \Psi_2 \\ & + \lambda_{R2} (\tilde{d}_R - \tilde{d}_R^\dagger) \Psi_1 + i\epsilon_M \Psi_1 \Psi_2, \end{aligned} \quad (1)$$

where the operators $\tilde{c}_{\alpha\mathbf{k}}^\dagger, \tilde{c}_{\alpha\mathbf{k}}$ correspond to electrons in the right and left metallic leads $\alpha = L, R$ having momentum \mathbf{k} and energy $\epsilon_{\alpha\mathbf{k}} = \epsilon_{\mathbf{k}} - \mu_{\alpha}$, with μ_{α} the corresponding chemical potential. The operators $\tilde{d}_{\alpha}^\dagger, \tilde{d}_{\alpha}$ describe the localized orbitals in the right and left QDs with energies $\tilde{\epsilon}_{\alpha}$, t_c is the hopping term corresponding to the normal direct tunneling between the QDs, which can lead to the formation of usual molecular orbitals [55], and \mathcal{V} describes the strength of the coupling between the QDs and the leads (we take it to be equal for right and left QDs). At the edges of the TSC wire, the nonlocal MBSs described by the operators $\Psi_j = \Psi_j^\dagger$ couple to the QDs with the amplitudes $\lambda_{\alpha j}$ with $j = 1, 2$ (the ratio $\eta_{\alpha} = |\lambda_{\alpha 1}/\lambda_{\alpha 2}|$ defines the nonlocality degree) and to each other via the overlap term ϵ_M .

The linear combination of the Majorana operators

$$f = \frac{1}{\sqrt{2}}(\Psi_1 + i\Psi_2) \quad (2)$$

forms a regular fermionic state.

Performing the rotation in *pseudospin* space $\sigma = \pm 1$ (\uparrow, \downarrow), with the two leads at the same chemical potential $\mu_L = \mu_R = 0$ [43], corresponding to R and L states, $\tilde{d}_L = \cos\theta d_\uparrow - \sin\theta d_\downarrow$, $\tilde{d}_R = \sin\theta d_\uparrow + \cos\theta d_\downarrow$, $\tilde{c}_{kL} = \cos\theta c_{k\uparrow} - \sin\theta c_{k\downarrow}$, and $\tilde{c}_{kR} = \sin\theta c_{k\uparrow} + \cos\theta c_{k\downarrow}$ with

$$\theta = \frac{\pi}{4} + \frac{1}{2} \arcsin \frac{\Delta\varepsilon}{\sqrt{4(t_c)^2 + (\Delta\varepsilon)^2}} \quad (3)$$

and $\Delta\varepsilon = \tilde{\varepsilon}_L - \tilde{\varepsilon}_R$, the Hamiltonian of the system can be rewritten as

$$\mathcal{H} = \sum_{\mathbf{k}\sigma} \varepsilon_{\mathbf{k}} c_{\mathbf{k}\sigma}^\dagger c_{\mathbf{k}\sigma} + \sum_{\sigma} \varepsilon_{d\sigma} d_{\sigma}^\dagger d_{\sigma} + \mathcal{V} \sum_{\mathbf{k}\sigma} (c_{\mathbf{k}\sigma}^\dagger d_{\sigma} + \text{H.c.}) + \varepsilon_M \left(f^\dagger f - \frac{1}{2} \right) + \sum_{\sigma} (\mathcal{V}_{\sigma}^- d_{\sigma} f^\dagger + \mathcal{V}_{\sigma}^+ d_{\sigma} f + \text{H.c.}), \quad (4)$$

where $\varepsilon_{d\sigma} = \frac{(\tilde{\varepsilon}_L + \tilde{\varepsilon}_R)}{2} - \frac{\sigma}{2} \sqrt{4(t_c)^2 + (\Delta\varepsilon)^2}$, $\mathcal{V}_{\uparrow}^{\mp} = \frac{1}{\sqrt{2}} [(\lambda_{R2} \mp \lambda_{R1}) \sin\theta + (\lambda_{L1} \mp \lambda_{L2}) \cos\theta]$, and $\mathcal{V}_{\downarrow}^{\mp} = \frac{1}{\sqrt{2}} [(\lambda_{R2} \mp \lambda_{R1}) \cos\theta - (\lambda_{L1} \mp \lambda_{L2}) \sin\theta]$.

The Hamiltonian given by Eq. (4) corresponds to the mapping of the original problem to one equivalent to a single spinor QD coupled to fermionic state f and characterized by the following mixture of states: the amplitudes $\mathcal{V}_{\uparrow(\downarrow)}^{\pm}$ correspond to the formation of delocalized Cooper pairs ($d_{\sigma} f$), while the terms $\mathcal{V}_{\uparrow(\downarrow)}^{\mp}$ give the normal couplings between the effective QD and f ($d_{\sigma} f^\dagger$).

By making explicit the *pseudospin* basis, we recognize the symmetric $d_\uparrow = \sin\theta \tilde{d}_R + \cos\theta \tilde{d}_L$ and antisymmetric $d_\downarrow = \cos\theta \tilde{d}_R - \sin\theta \tilde{d}_L$ superpositions as the bonding and antibonding molecular states, respectively, due to the linear combination of atomic orbitals (LCAO) between \tilde{d}_L and \tilde{d}_R . Strictly for $t_c = 0$, note that from Eq. (3), $\theta = \frac{\pi}{2}$ ($\theta = 0$) when $\Delta\varepsilon \rightarrow 0^+$ ($\Delta\varepsilon \rightarrow 0^-$) leading to the breaking down of the LCAO. As we are interested in the pairing dominated by the MBSs, in the following discussion we will consider the case of identical QDs that are weakly coupled. It corresponds to $\tilde{\varepsilon}_L = \tilde{\varepsilon}_R = \varepsilon_d$ and $t_c \rightarrow 0$, but finite as in Ref. [58], thus giving rise to $\theta = \frac{\pi}{4}$ as shown in Fig. 2(a) of Sec. III, where we present the profile of Eq. (3) as a function of $\Delta\varepsilon$ for several t_c values.

The QD states corresponding to the opposite *pseudospins* are now simply symmetric and antisymmetric combinations between the orbitals of right and left QDs:

$$d_\uparrow = \frac{\tilde{d}_R + \tilde{d}_L}{\sqrt{2}} \quad \text{and} \quad d_\downarrow = \frac{\tilde{d}_R - \tilde{d}_L}{\sqrt{2}}, \quad (5)$$

which represent the bonding and antibonding molecular states with the energies $\varepsilon_{d\sigma} = \varepsilon_d - \sigma t_c$, respectively. Moreover,

$$\mathcal{V}_{\uparrow}^{\mp} = \frac{\lambda_{R2} + \lambda_{L1} \mp (\lambda_{R1} + \lambda_{L2})}{2} \quad (6)$$

and

$$\mathcal{V}_{\downarrow}^{\mp} = \frac{\lambda_{R2} - \lambda_{L1} \mp (\lambda_{R1} - \lambda_{L2})}{2}. \quad (7)$$

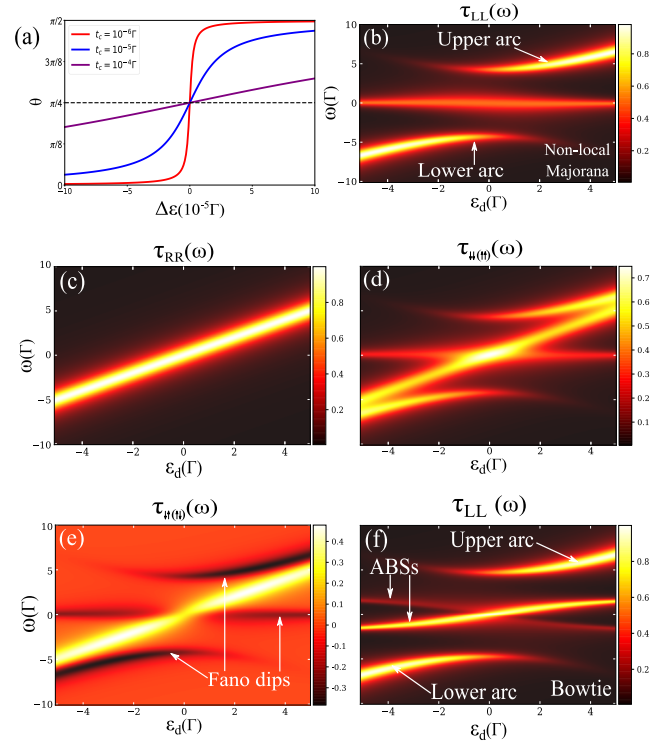


FIG. 2. *The Majorana molecule turned-off scenario.* Color maps of the spectral density of the QDs spanned by ω and $\varepsilon_d = \tilde{\varepsilon}_L = \tilde{\varepsilon}_R$. Panel (a) shows Eq. (3) for θ as a function of $\Delta\varepsilon$, which points out that for two identical weakly coupled QDs ($t_c \rightarrow 0$, but finite as in Ref. [58]), Eq. (4) should be evaluated at $\theta = \frac{\pi}{4}$. Panels (b)–(e) correspond to the case of a right QD weakly coupled to the MBSs, $\lambda_{L1} = 3\Gamma$ and $t_c = \lambda_{L2} = \lambda_{R1} = \lambda_{R2} = \varepsilon_M = 10^{-5}\Gamma$. In panel (b) the density plot of $\tau_{LL}(\omega)$ demonstrates a clearly visible horizontal bright line, corresponding to the ZBP due to the coupling with the MBS Ψ_1 , which is robust against changes in ε_d [27]. In panel (c) the spectral density $\tau_{RR}(\omega)$ reveals solely the resonant level of the right QD, weakly coupled to the MBSs at $\omega = \varepsilon_d$. In this regime, Fano interference between the QDs is absent, and $\tau_{RL}(\omega) = \tau_{LR}(\omega) = 0$. Panels (d) and (e) show $\tau_{\uparrow\uparrow}(\omega) = \tau_{\downarrow\downarrow}(\omega)$ and $\tau_{\uparrow\downarrow}(\omega) = \tau_{\downarrow\uparrow}(\omega)$, respectively, which reveal clear signatures of constructive and destructive Fano interference. Panel (f) accounts for the coupling of the left QD to the overlapping MBSs ($\lambda_{L1} = 3\Gamma$, $\lambda_{L2} = 0.001\Gamma$, $t_c = \lambda_{R1} = \lambda_{R2} = 10^{-5}\Gamma$, and $\varepsilon_M = 2\Gamma$). In this case, the density plot for τ_{LL} reveals the transformation of the horizontal bright line, corresponding to the ZBP, into a *bowtie* profile, characteristic for split ABSs [23].

As we will see, the communication between the QDs leads to the splitting of the ABSs into ABS- \uparrow and ABS- \downarrow , and the formation of a Majorana molecule.

We characterize the QDs by their normalized spectral densities

$$\tau_{jl}(\omega) = -\Gamma \text{Im}(\langle\langle d_j; d_l^\dagger \rangle\rangle), \quad (8)$$

where $j, l = L, R$, $\langle\langle d_j; d_l^\dagger \rangle\rangle$ are retarded Green's functions (GFs) in the frequency domain, and $\Gamma = \pi \mathcal{V}^2 \sum_{\mathbf{k}} \delta(\varepsilon - \varepsilon_{\mathbf{k}})$ [59]. We highlight that Eq. (8) is temperature-independent once in the system Hamiltonian of Eq. (1) the Coulomb correlation $U \tilde{d}_L^\dagger \tilde{d}_L \tilde{d}_R^\dagger \tilde{d}_R$, which corresponds to $U d_\uparrow^\dagger d_\downarrow^\dagger d_\downarrow d_\uparrow$ in

Eq. (4), is suppressed by the superconducting wire between the QDs, as discussed in Ref. [58]. Otherwise, the interdot correlation would induce the Kondo effect [43]. Performing the *pseudospin* rotation given by Eq. (5), we get

$$\tau_{LL(RR)}(\omega) = \frac{1}{2}\{(\tau_{\uparrow\uparrow} + \tau_{\downarrow\downarrow}) \mp (\tau_{\uparrow\downarrow} + \tau_{\downarrow\uparrow})\} \quad (9)$$

and

$$\tau_{RL(LR)}(\omega) = \frac{1}{2}\{(\tau_{\uparrow\uparrow} - \tau_{\downarrow\downarrow}) \mp (\tau_{\uparrow\downarrow} - \tau_{\downarrow\uparrow})\} \quad (10)$$

for the local and nonlocal QD densities, respectively. The presence of the terms $\tau_{\uparrow\downarrow}$ ($\tau_{\downarrow\uparrow}$) accounts for the Fano interference in the *pseudospin* channels. Conversely, the QDs \tilde{d}_L and \tilde{d}_R interfere with each other, thus forming $\tau_{\uparrow\uparrow}(\omega)$ (bonding) and $\tau_{\downarrow\downarrow}(\omega)$ (antibonding) orbitals

$$\tau_{\uparrow\uparrow(\downarrow\downarrow)}(\omega) = \frac{1}{2}\{(\tau_{LL} + \tau_{RR}) \pm (\tau_{RL} + \tau_{LR})\} \quad (11)$$

and

$$\tau_{\uparrow\downarrow(\downarrow\uparrow)}(\omega) = \frac{1}{2}\{(\tau_{RR} - \tau_{LL}) \pm (\tau_{LR} - \tau_{RL})\}. \quad (12)$$

As the left and right metallic leads should have the same chemical potentials ($\mu_L = \mu_R = 0$ [43]) for the emergence of the *pseudospin* scenario of Eq. (4), the differential conductance \mathcal{G} at a finite bias-voltage eV cannot be measured through these leads. Thus, the experimental detection of the spectral densities given by Eqs. (9) and (11) needs an extra electron reservoir. To that end, the transport can be observed by employing an STM-tip perturbatively coupled to the 1D-TSC and QDs, as proposed in Fig. 1(a) and Ref. [29]. In such an apparatus, by considering the temperature $T \rightarrow 0$ K ($k_B T \ll \Gamma$, where k_B is the Boltzmann constant and $\Gamma = 40 \mu\text{eV}$ [27] as the system energy scale) and low bias-voltage $eV \rightarrow 0$ ($eV \ll \Gamma$), $\mathcal{G} \propto \int d\omega \text{LDOS}(\omega) \{-\frac{\partial}{\partial e} n_F(\omega - eV)\} \approx \text{LDOS}(eV)$, with n_F as the Fermi-Dirac distribution and $\{-\frac{\partial}{\partial e} n_F(\omega - eV)\} \approx \delta(\omega - eV)$. This means that the conductance becomes ruled by the local density of states (LDOS) evaluated at the tip chemical potential $\mu_{\text{tip}} = eV = \omega$. For the STM-tip placed over the left (right) QD, the LDOS behavior will be determined by $\tau_{LL}(\omega)$ [$\tau_{RR}(\omega)$], but upon varying the tip position over the wire, the LDOS is expected to catch traces of the interfering processes through the QDs, such as those present in $\tau_{\uparrow\uparrow}(\omega)$ [56,57]. In this manner, the STM-tip becomes naturally *pseudospin*-resolved. We clarify that the quantitative evaluation of the LDOS spatial dependence along the 1D-TSC is not the focus of the current work once it requires us to adopt the Kitaev chain explicitly in the approach.

To evaluate $\langle\langle d_\sigma; d_\sigma^\dagger \rangle\rangle$, we apply the equation-of-motion method [60] to Eq. (4), which gives

$$(\omega + i0^+) \langle\langle d_\sigma; d_\sigma^\dagger \rangle\rangle = \delta_{\sigma\sigma'} + \langle\langle [d_\sigma, \mathcal{H}]; d_\sigma^\dagger \rangle\rangle. \quad (13)$$

The last term in Eq. (13) will generate the anomalous Green functions $\langle\langle d_\sigma^\dagger; d_\sigma^\dagger \rangle\rangle$. As the Hamiltonian is quadratic, the system of equations can be closed and written in matrix form as $A^\sigma(\omega) \langle\langle (d_\sigma; d_\sigma^\dagger) \quad (d_{\bar{\sigma}}; d_{\bar{\sigma}}^\dagger) \quad (d_\sigma^\dagger; d_\sigma) \quad (d_{\bar{\sigma}}^\dagger; d_{\bar{\sigma}}) \rangle\rangle^T =$

$(1 \ 0 \ 0 \ 0)^T$, with

$$A^\sigma(\omega) = \begin{bmatrix} a_\sigma(\omega) & -k_{2-}^{\sigma\bar{\sigma}}(\omega) & k_{1-}^{\sigma\sigma}(\omega) & k_{1-}^{\sigma\bar{\sigma}}(\omega) \\ -k_{2-}^{\bar{\sigma}\sigma}(\omega) & a_{\bar{\sigma}}(\omega) & k_{1-}^{\bar{\sigma}\sigma}(\omega) & k_{1-}^{\bar{\sigma}\bar{\sigma}}(\omega) \\ k_{1+}^{\sigma\sigma}(\omega) & k_{1+}^{\sigma\bar{\sigma}}(\omega) & b_\sigma(\omega) & -k_{2+}^{\sigma\bar{\sigma}}(\omega) \\ k_{1+}^{\bar{\sigma}\sigma}(\omega) & k_{1+}^{\bar{\sigma}\bar{\sigma}}(\omega) & -k_{2+}^{\bar{\sigma}\sigma}(\omega) & b_{\bar{\sigma}}(\omega) \end{bmatrix}, \quad (14)$$

where $\bar{\sigma} = -\sigma$, $k_{1\mp}^{\sigma\sigma'}(\omega) = \mathcal{V}_\sigma^- \mathcal{V}_{\sigma'}^+(\omega \mp \varepsilon_M)^{-1} + \mathcal{V}_\sigma^- \mathcal{V}_{\sigma'}^+(\omega \pm \varepsilon_M)^{-1}$, $k_{2\mp}^{\sigma\sigma'}(\omega) = \mathcal{V}_\sigma^- \mathcal{V}_{\sigma'}^-(\omega \mp \varepsilon_M)^{-1} + \mathcal{V}_\sigma^+ \mathcal{V}_{\sigma'}^+(\omega \pm \varepsilon_M)^{-1}$, $a_\sigma(\omega) = \omega - \varepsilon_{d\sigma} - k_{2-}^{\sigma\sigma} + i\Gamma$, and $b_\sigma(\omega) = \omega + \varepsilon_{d\sigma} - k_{2+}^{\sigma\sigma} + i\Gamma$.

III. RESULTS AND DISCUSSION

We assume $\Gamma = 40 \mu\text{eV}$ [27] as the energy scale of the model parameters of the system. In Fig. 2(a) we present Eq. (3) as a function of $\Delta\varepsilon$, which shows that the *pseudospin* mapping is applied to $\theta = \frac{\pi}{4}$ when $t_c \rightarrow 0$, but it is finite for the experimental condition $\Delta\varepsilon = 0$. This point defines the scenario adopted in this work for the evaluation of the spectral analysis.

Our aim is to investigate the spectral function of the considered system defined by Eq. (8). To better understand the situation qualitatively, we start from the geometry wherein only the left QD is strongly coupled to MBSs, i.e., from the Majorana molecule turned-off scenario. We present the results for both the case of a highly nonlocal MBS [27] [Fig. 2(b)] and the case of overlapping MBSs [Fig. 2(f)]. For both cases we present the 2D plots of the spectral functions in the ω and ε_d axes.

Figure 2(b) shows the spectral function corresponding to the left QD, $\tau_{LL}(\omega)$ in the situation, when it is strongly coupled only to the closest MBS ($\lambda_{L1} = 3\Gamma$ and $t_c = \lambda_{R1} = \lambda_{R2} = \lambda_{L2} = \varepsilon_M = 10^{-5}\Gamma$). In perfect agreement with Ref. [27], one can see the bright plateau at $\omega = 0$, corresponding to the ZBP in the conductance, which is robust against the ε_d perturbations and is provided by the presence of highly nonlocal MBSs. The upper and lower arcs correspond to the QD states split by the coupling to the MBS Ψ_1 . Naturally, as the right QD is weakly coupled to both MBSs, its spectral function $\tau_{RR}(\omega)$, shown in Fig. 2(c), is trivial and consists of a single peak corresponding to $\omega = \varepsilon_d$. As the QDs do not communicate through the 1D-TSC, $\tau_{RL}(\omega) = \tau_{LR}(\omega) = 0$.

In the *pseudospin* basis, the latter condition, according to Eqs. (6), (7), (11), and (12), imposes *pseudospin* degeneracy, so that $\tau_{\uparrow\uparrow}(\omega) = \tau_{\downarrow\downarrow}(\omega)$ [shown in Fig. 2(d)] and $\tau_{\uparrow\downarrow}(\omega) = \tau_{\downarrow\uparrow}(\omega)$ [Fig. 2(e)], $|\mathcal{V}_\uparrow^+| = |\mathcal{V}_\downarrow^-|$ and $|\mathcal{V}_\uparrow^-| = |\mathcal{V}_\downarrow^+|$, and, in addition, $|\mathcal{V}_\sigma^-| = |\mathcal{V}_\sigma^+|$. *Pseudospin* degeneracy, in particular, means that both Cooper pairings in the *pseudospin* channels given by $d_\uparrow f$ and $d_\downarrow f$ contribute to the Hamiltonian on an equal footing. The fact that $\tau_{\uparrow\downarrow}(\uparrow\downarrow)(\omega) \neq 0$ means that two *pseudospin* channels, corresponding to bonding and antibonding states, are nonorthogonal, and thus a Majorana molecule is not formed. Spectral functions in the *pseudospin* basis are presented in Figs. 2(d) and 2(e), and they reveal clear signatures of the Fano interference peaks and dips.

If one accounts for the coupling of the left QD to the MBS Ψ_2 ($\lambda_{L2} = 0.001\Gamma$), with finite overlap between the states Ψ_1

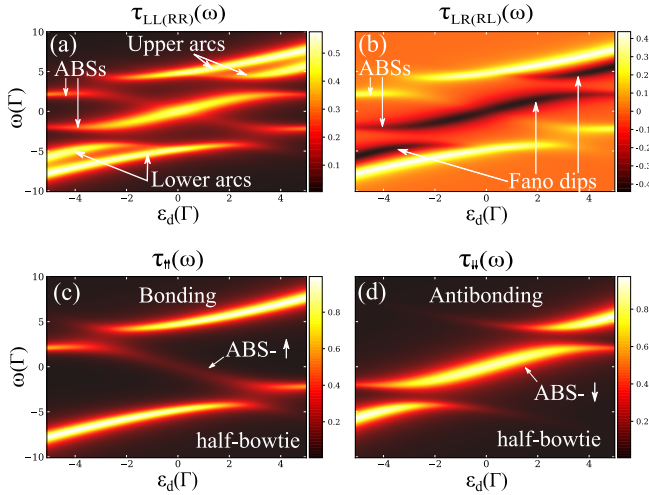


FIG. 3. *The Majorana molecule turned-on scenario.* Color maps of the spectral density of the QDs spanned by ω and $\epsilon_d = \tilde{\epsilon}_L = \tilde{\epsilon}_R$. The parameters of the system are $t_c = 10^{-5}\Gamma$, $\lambda_{L1} = \lambda_{R1} = 3\Gamma$, $\lambda_{L2} = \lambda_{R2} = 1.5\Gamma$, and $\epsilon_M = 0.05\Gamma$. Panel (a) shows the profiles of $\tau_{LL}(\omega) = \tau_{RR}(\omega)$, and reveals the splitting of the upper and lower arcs due to the formation of the bonding (ABS- \uparrow) and antibonding (ABS- \downarrow) Andreev molecular states. The *pseudospin* lifting in $\tau_{\uparrow\uparrow(\downarrow\downarrow)}(\omega)$ is attributed to the Fano interference between $\tau_{LL(RR)}(\omega)$ and $\tau_{LR(RL)}(\omega)$, which appears in panel (b). The formation of the aforementioned molecular states is even more clearly visible in panels (c) and (d), corresponding to $\tau_{\uparrow\uparrow}(\omega)$ and $\tau_{\downarrow\downarrow}(\omega)$, where the novel *half-bowtie*-like structures are formed. In this regime $\tau_{\downarrow\downarrow}(\omega) = \tau_{\uparrow\uparrow}(\omega) = 0$, and Majorana molecular states are resolved in the *pseudospin* basis.

and Ψ_2 ($\epsilon_M = 2\Gamma$), but keeps the right QD weakly coupled ($t_c = \lambda_{R1} = \lambda_{R2} = 10^{-5}\Gamma$), the spectral function $\tau_{LL}(\omega)$ reveals a characteristic *bowtie* profile [23,28] (also referred to as a double fork [36]) instead of a robust ZBP. This corresponds to the presence in the system of a pair of trivial ABSs, as is shown in Fig. 2(f). Other spectral functions remain qualitatively the same. The condition of *pseudospin* degeneracy still holds, and a Majorana molecule is not formed.

Now, we can consider the symmetric case sketched in Fig. 1(a) with $t_c = 10^{-5}\Gamma$, $\lambda_{L1} = \lambda_{R1} = 3\Gamma$, $\lambda_{L2} = \lambda_{R2} = 1.5\Gamma$, and $\epsilon_M = 0.05\Gamma$, corresponding to *the Majorana molecule turned-on scenario*: both QDs are coupled to both MBSs, and thus they interfere with each other through the 1D-TSC. In this situation, a *bowtie*-like signature emerges in the spectral density $\tau_{LL(RR)}(\omega)$, as can be seen from Fig. 3(a). Moreover, the features characteristic of usual molecular binding can be seen, as upper and lower arcs provided by the

coupling of the QD states, visible in Fig. 2(f), become split in Fig. 3(a) due to the TSC-mediated overlap of the states of right and left QDs. Naturally, this leads to $\tau_{RL}(\omega) = \tau_{LR}(\omega) \neq 0$ [see Fig. 3(b)], which, according to Eqs. (11) and (12), means that $\tau_{\uparrow\uparrow}(\omega) \neq \tau_{\downarrow\downarrow}$ and $\tau_{\downarrow\uparrow(\uparrow\downarrow)}(\omega) = 0$.

Physically, this means that spin-up and spin-down channels become decoupled in the *pseudospin* basis, and a Majorana molecule, which is a bonding or antibonding superposition of ABSs, is formed. The latter manifest themselves in the spectral profiles of $\tau_{\uparrow\uparrow}(\omega)$ and $\tau_{\downarrow\downarrow}(\omega)$ shown in Figs. 3(c) and 3(d), respectively, as *half-bowtie* signatures. They are consequences of the Fano interference between $\tau_{LR}(\omega)$ and $\tau_{RL}(\omega)$, shown in Fig. 3(b). Note that the latter contains both peaks and pronounced Fano dips, which interfere constructively or destructively depending on the sign in Eqs. (11) and (12), with the peaks in the spectral densities of $\tau_{LL}(\omega)$ and $\tau_{RR}(\omega)$, which gives in the end the mentioned *half-bowtie* profiles.

In terms of the effective Hamiltonian [Eq. (4)], the considered regime corresponds to the case when $|\mathcal{V}_\uparrow^-| \neq 0$, $|\mathcal{V}_\uparrow^+| = 0$, $|\mathcal{V}_\downarrow^-| = 0$, and $|\mathcal{V}_\downarrow^+| \neq 0$. This means that only the *pseudospin* Cooper pairing $d_\uparrow f$ and normal electron tunneling $d_\downarrow f^\dagger$ contribute to the transport assisted by the formation of Majorana molecules.

IV. CONCLUSIONS

In summary, we have proposed the concept of a Majorana molecule, a bonding or antibonding state appearing in the system of a pair of QDs flanking a 1D-TSC nanowire. The coupling between QDs is achieved via the channel provided by the presence of MBSs. It is demonstrated that these states manifest themselves via *half-bowtie* spectral fingerprints in the spectral density of states, which are qualitatively different from full *bowtie* profiles, characteristic of the case of a single QD. Such features can be measured by an STM-tip, which becomes naturally *pseudospin* resolved, once the QDs behave as a nonlocal two-probe detector of the Fano interference assisted by the MBSs.

ACKNOWLEDGMENTS

We thank the Brazilian funding agencies CNPq (Grants No. 305668/2018-8 and No. 302498/2017-6), the São Paulo Research Foundation (FAPESP; Grant No. 2015/23539-8), and Coordenação de Aperfeiçoamento de Pessoal de Nível Superior–Brasil (CAPES)–Finance Code 001. Y.M. and I.A.S. acknowledge support from the Government of the Russian Federation through the Megagrant 14.Y26.31.0015 and ITMO 5-100 Program.

- [1] R. Aguado, *Riv. Nuovo Cimento* **40**, 523 (2017).
- [2] C. Nayak, S. H. Simon, A. Stern, M. Freedman, and S. Das Sarma, *Rev. Mod. Phys.* **80**, 1083 (2008).
- [3] J. Alicea, *Rep. Prog. Phys.* **75**, 076501 (2012).
- [4] S. R. Elliott and M. Franz, *Rev. Mod. Phys.* **87**, 137 (2015).
- [5] G. Goldstein and C. Chamon, *Phys. Rev. B* **84**, 205109 (2011).

- [6] J. C. Budich, S. Walter, and B. Trauzettel, *Phys. Rev. B* **85**, 121405(R) (2012).
- [7] A. Y. Kitaev, *Phys. Usp.* **44**, 131 (2001).
- [8] H. Zhang, C.-X. Liu, S. Gazibegovic, D. Xu, J. A. Logan, G. Wang, N. van Loo, J. D. S. Bommer, M. W. A. de Moor, D. Car, R. L. M. Op het Veld, P. J. van Veldhoven, S. Koelling,

- M. A. Verheijen, M. Pendharkar, D. J. Pennachio, B. Shojaei, J. S. Lee, C. J. Palmstrom, E. P. A. M. Bakkers, S. D. Sarma, and L. P. Kouwenhoven, *Nature (London)* **556**, 74 (2018).
- [9] T.-P. Choy, J. M. Edge, A. R. Akhmerov, and C. W. J. Beenakker, *Phys. Rev. B* **84**, 195442 (2011).
- [10] S. Nadj-Perge, I. K. Drozdov, B. A. Bernevig, and A. Yazdani, *Phys. Rev. B* **88**, 020407(R) (2013).
- [11] J. Klinovaja, P. Stano, A. Yazdani, and D. Loss, *Phys. Rev. Lett.* **111**, 186805 (2013).
- [12] B. Braunecker and P. Simon, *Phys. Rev. Lett.* **111**, 147202 (2013).
- [13] M. M. Vazifeh and M. Franz, *Phys. Rev. Lett.* **111**, 206802 (2013).
- [14] F. Pientka, L. I. Glazman, and F. von Oppen, *Phys. Rev. B* **88**, 155420 (2013).
- [15] S. Nadj-Perge, I. K. Drozdov, J. Li, H. Chen, S. Jeon, J. Seo, A. H. MacDonald, B. A. Bernevig, and A. Yazdani, *Science* **346**, 602 (2014).
- [16] R. Pawlak, M. Kisiel, J. Klinovaja, T. Meier, S. Kawai, T. Glatzel, D. Loss, and E. Meyer, *Quantum Inf.* **2**, 16035 (2016).
- [17] S. Jeon, Y. Xie, J. Li, Z. Wang, B. A. Bernevig, and A. Yazdani, *Science* **358**, 772 (2017).
- [18] M. Ruby, B. W. Heinrich, Y. Peng, F. von Oppen, and K. J. Franke, *Nano Lett.* **17**, 4473 (2017).
- [19] P. Marra and M. Nitta, *Phys. Rev. B* **100**, 220502(R) (2019).
- [20] V. Mourik, K. Zuo, S. M. Frolov, S. R. Plissard, E. P. A. M. Bakkers, and L. P. Kouwenhoven, *Science* **336**, 1003 (2012).
- [21] S. M. Albrecht, A. Higginbotham, M. Madsen, F. Kuemmeth, T. S. Jespersen, J. Nygard, P. Krogstrup, and C. Marcus, *Nature (London)* **531**, 206 (2016).
- [22] M.-T. Deng, S. Vaitiekėnas, E. B. Hansen, J. Danon, M. Leijnse, K. Flensberg, J. Nygard, P. Krogstrup, and C. M. Marcus, *Science* **354**, 1557 (2016).
- [23] M.-T. Deng, S. Vaitiekėnas, E. Prada, P. San-Jose, J. Nygard, P. Krogstrup, R. Aguado, and C. M. Marcus, *Phys. Rev. B* **98**, 085125 (2018).
- [24] L. Fu and C. L. Kane, *Phys. Rev. Lett.* **100**, 096407 (2008).
- [25] S. Zhu, L. Kong, L. Cao, H. Chen, M. Papaj, S. Du, Y. Xing, W. Liu, D. Wang, C. Shen, F. Yang, J. Schneeloch, R. Zhong, G. Gu, L. Fu, Y.-Y. Zhang, H. Ding, and H.-J. Gao, *Science* **367**, 189 (2020).
- [26] D. E. Liu and H. U. Baranger, *Phys. Rev. B* **84**, 201308(R) (2011).
- [27] E. Vernek, P. H. Penteado, A. C. Seridonio, and J. C. Egues, *Phys. Rev. B* **89**, 165314 (2014).
- [28] E. Prada, R. Aguado, and P. San-Jose, *Phys. Rev. B* **96**, 085418 (2017).
- [29] A. Ptok, A. Kobialka, and T. Domanski, *Phys. Rev. B* **96**, 195430 (2017).
- [30] D. E. Liu, A. Levchenko, and R. M. Lutchyn, *Phys. Rev. B* **92**, 205422 (2015).
- [31] D. E. Liu, M. Cheng, and R. M. Lutchyn, *Phys. Rev. B* **91**, 081405(R) (2015).
- [32] S. Smirnov, *New J. Phys.* **19**, 063020 (2017).
- [33] S. Smirnov, *Phys. Rev. B* **99**, 165427 (2019).
- [34] L. Hong, F. Chi, Z.-G. Fu, Y.-F. Hou, Z. Wang, K.-M. Li, J. Liu, H. Yao, and P. Zhang, *Appl. Phys.* **127**, 124302 (2020).
- [35] F. Chi, Z.-G. Fu, J. Liu, K.-M. Li, Z. Wang, and P. Zhang, *Nanoscale Res. Lett.* **15**, 79 (2020).
- [36] L. S. Ricco, F. A. Dessotti, I. A. Shelykh, M. S. Figueira, and A. C. Seridonio, *Sci. Rep.* **8**, 2790 (2018).
- [37] J. D. Cifuentes and L. G. G. V. Dias da Silva, *Phys. Rev. B* **100**, 085429 (2019).
- [38] L. H. Guessi, F. A. Dessotti, Y. Marques, L. S. Ricco, G. M. Pereira, P. Menegasso, M. de Souza, and A. C. Seridonio, *Phys. Rev. B* **96**, 041114(R) (2017).
- [39] U. Fano, *Phys. Rev.* **124**, 1866 (1961).
- [40] A. E. Miroshnichenko, S. Flach, and Y. S. Kivshar, *Rev. Mod. Phys.* **82**, 2257 (2010).
- [41] H.-W. Lee and S. Kim, *Phys. Rev. Lett.* **98**, 186805 (2007).
- [42] V. Kashcheyevs, A. Schiller, A. Aharony, and O. Entin-Wohlman, *Phys. Rev. B* **75**, 115313 (2007).
- [43] Q.-F. Sun and H. Guo, *Phys. Rev. B* **66**, 155308 (2002).
- [44] S. Amasha, A. J. Keller, I. G. Rau, A. Carmi, J. A. Katine, H. Shtrikman, Y. Oreg, and D. Goldhaber-Gordon, *Phys. Rev. Lett.* **110**, 046604 (2013).
- [45] A. Schuray, L. Weithofer, and P. Recher, *Phys. Rev. B* **96**, 085417 (2017).
- [46] A. Ueda and T. Yokoyama, *Phys. Rev. B* **90**, 081405(R) (2014).
- [47] J.-J. Xia, S.-Q. Duan, and W. Zhang, *Nanoscale Res. Lett.* **10**, 223 (2015).
- [48] C. Jiang and Y.-S. Zheng, *Solid State Commun.* **212**, 14 (2015).
- [49] Q.-B. Zeng, S. Chen, L. You, and R. Lu, *Front. Phys.* **12**, 127302 (2016).
- [50] Y. Xiong, *Chin. Phys. Lett.* **33**, 057402 (2016).
- [51] J. Baranski, A. Kobialka, and T. Domanski, *J. Phys.: Condens. Matter* **29**, 075603 (2016).
- [52] X.-Q. Wang, S.-F. Zhang, C. Jiang, G.-Y. Yi, and W.-J. Gong, *Physica E* **104**, 1 (2018).
- [53] J. P. R.-Andrade, D. Zambrano, and P. A. Orellana, *An. Phys.* **531**, 1800498 (2019).
- [54] L. S. Ricco, V. L. Campo, I. A. Shelykh, and A. C. Seridonio, *Phys. Rev. B* **98**, 075142 (2018).
- [55] H. Lu, R. Lu, and B.-F. Zhu, *Phys. Rev. B* **71**, 235320 (2005).
- [56] Y. Marques, W. N. Mizobata, R. S. Oliveira, M. de Souza, M. S. Figueira, I. A. Shelykh, and A. C. Seridonio, *Sci. Rep.* **9**, 8452 (2019).
- [57] Y. Marques, A. E. Obispo, L. S. Ricco, M. de Souza, I. A. Shelykh, and A. C. Seridonio, *Phys. Rev. B* **96**, 041112(R) (2017).
- [58] M. Leijnse and K. Flensberg, *Phys. Rev. B* **86**, 134528 (2012).
- [59] P. W. Anderson, *Phys. Rev.* **124**, 41 (1961).
- [60] H. Bruus and K. Flensberg, *Many-Body Quantum Theory in Condensed Matter Physics, An Introduction* (Oxford University Press, Oxford, 2012).